ELM burn-through simulations for MAST-U Super-X plasmas

UNIVERSITY of York

UK Atomic Energy Authority

S.F. Smith[1], S.J.P. Pamela[1], A. Fil[1], M. Hölzl[2], G.T.A. Huijsmans[3,4], A.Kirk[1], D. Moulton[1], O. Myatra[1,5], A.J. Thornton[1], H.R. Wilson[5] and the JOREK team[a)]

[1] CCFE-UKAEA, Culham Science Centre, Abingdon, UK. [2] Max Planck Institute for Plasma Physics Garching .b M., Germany. [3] CEA, IRFM Saint-Paul-Lea-Durance, France. [4] Eindhoven University of Technology, Eindhoven, Netherlands. [5] York Plasma Institute York, United Kingdom.

[a)] See M Hoelzl, GTA Huijsmans, SJP Pamela, M Becoulet, E Nardon, FJ Artola, B Nkonga, et al The JOREK non-linear extended MHD code and applications to large-scale instabilities and their control in magnetically confined fusion plasmas Nuclear Fusion (submitted); preprint at: arXiv:2011.09120 for the present list of team members.

1) Introduction

✦ New Super-X divertor will be tested in MAST-U [1] to reduce target heat fluxes

✦ Plasma detachment predicted in MAST-U Super-X L-mode [2] and H-mode [3] plasmas

✦ Behaviour during ELMy H-mode, in Super-X, is unknown and investigated here

✦ ELM burn-through questions can only be answered with confidence when MAST-U experimental data is analysed

✦ **JOREK** [4,5,6] is used for first simulations of ELMs in MAST-U Super-X. Model given in [7]

2) Divertor comparison

✦ Conventional to Super-X, same profiles (based on MAST case [8]), with different divertor leg lengths (Fig. 1. a)-e))

✦ Single mode (n=20) simulation for R1-R5

✦ Conventional to Super-X peak heat flux (q_{peak}) reduces by factor 11, which is reasonable considering target area change

✦ ELM fluence ($\varepsilon_{||}$) along target in Fig. 1. f) for R1-R5

✦ Peak $\varepsilon_{||}$ deviates from scaling [9] for Super-X, Fig. 1. g), $\varepsilon_{||}$ is factor 22 lower for R5 (blue triangle) than scaling

✦ Results indicate ELM is partially buffered if the divertor is in a Super-X configuration and/or a detached regime prior to ELM (black diamond Fig. 1. g))

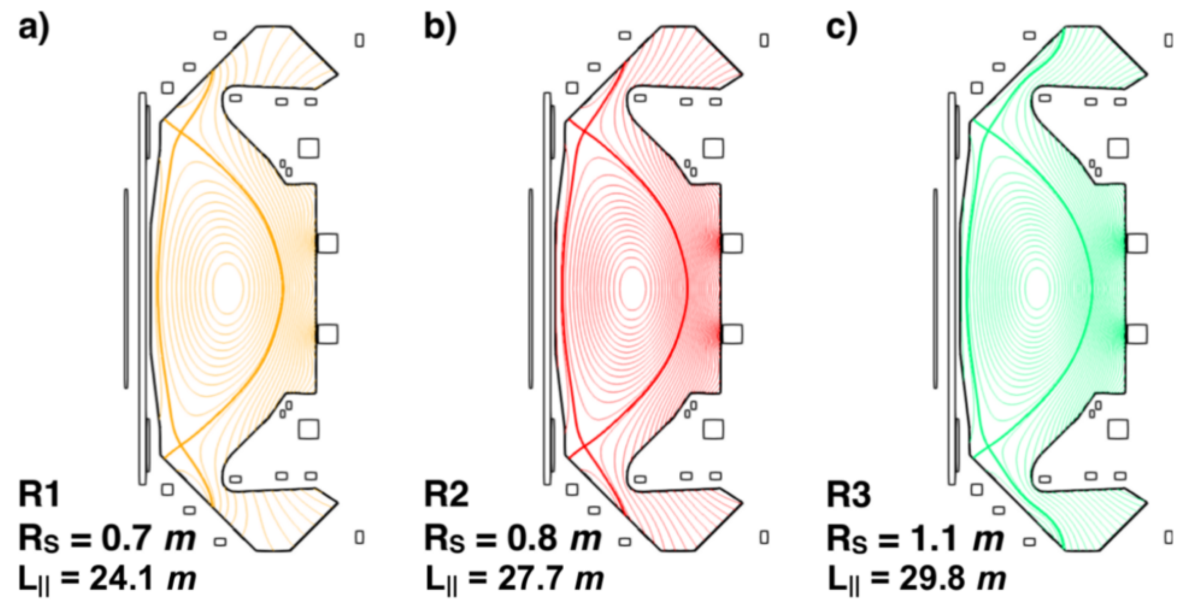

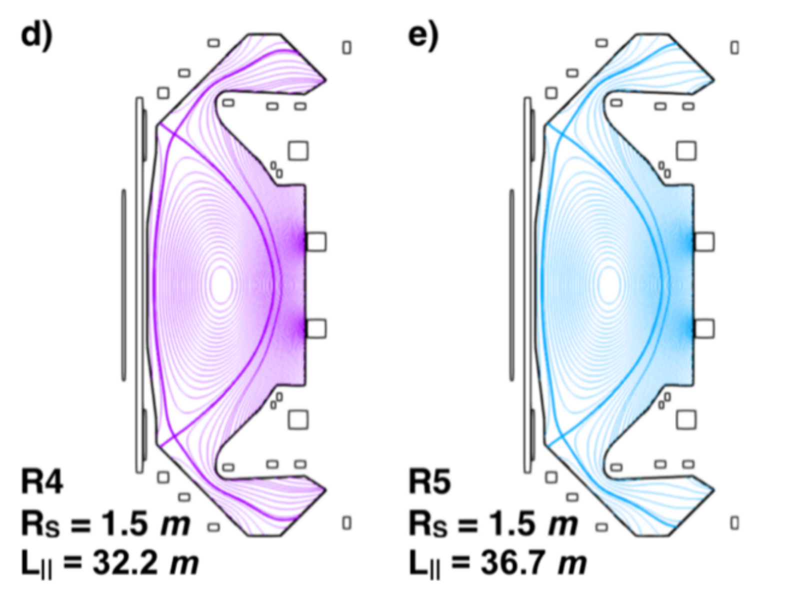

ELM growth rate similar for each case ~ 3.4×10^4 s^{-1}

ELM pedestal losses similar for R1 to R5

- Energy ~ 0.8 kJ (10.4%)
- Particles ~ 1.1×10^{19} (12.8%)

Peak heat flux reduction
8 to 0.7 MW/m^2 from R1 to R5

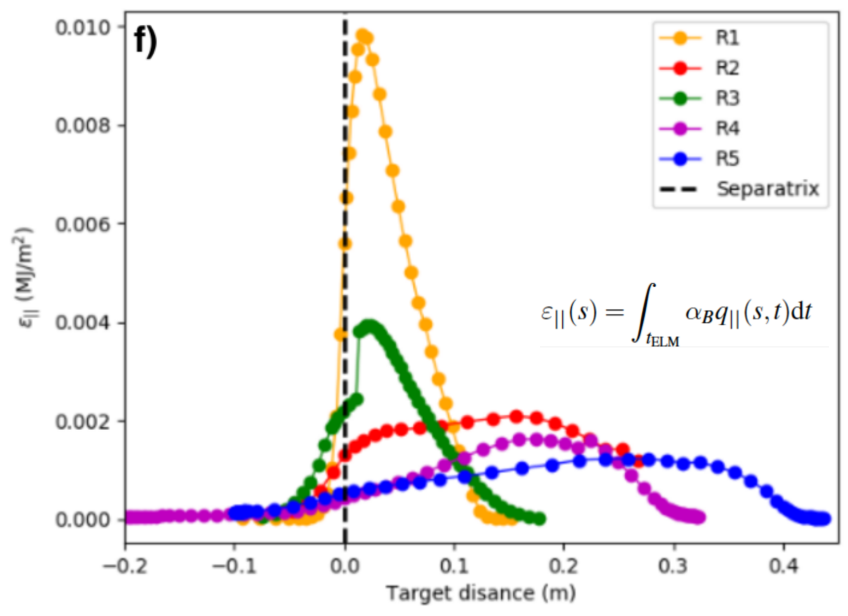

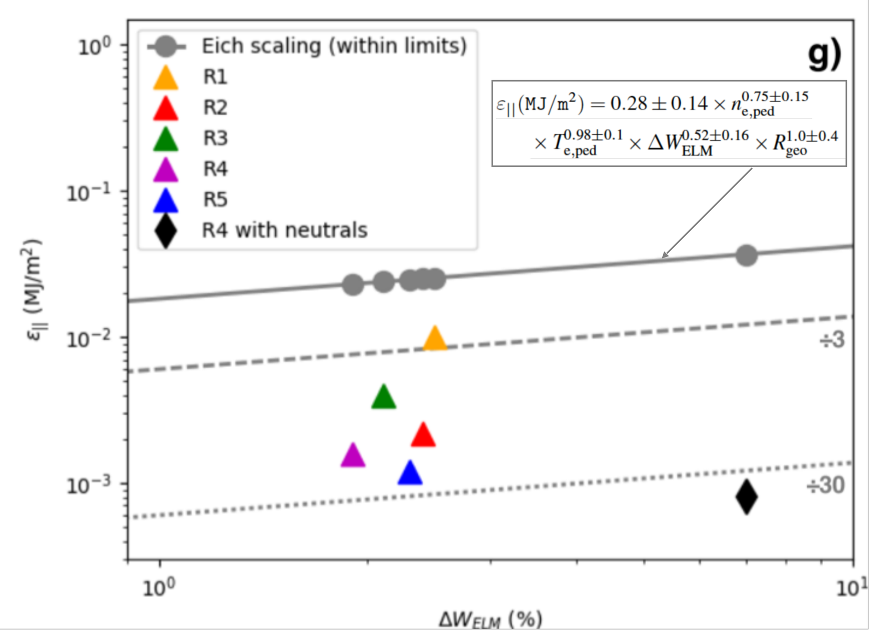

FIG. 1. Poloidal plane flux contour plots for a conventional MAST-U divertor (a) extending the outer leg (b) and (c) towards a Super-X divertor. The Super-X configuration (d) with no flux expansion in the divertor chambers and (e) with flux expansion. The black boxes indicate the coil positions and the thicker coloured lines show each separatrix. R_s is the strike point radius and $L_{||}$ is the connection length from mid-plane to target at Ψ_n =1.0001. (f) Profiles of the ELM energy fluence ($\varepsilon_{||}$) as a function of target distance for each of the divertor configurations. (g) The peak ELM parallel energy fluence as a function of ELM energy loss (note axes in log scale). $\varepsilon_{||}$ is given for Eich ELM scaling (from [9]) within regression limits given by grey circles. The coloured triangles represent the different divertor configurations and the black diamond indicates the Super-X case run with the neutrals model.

3) JOREK divertor detachment

✦ Detached divertor first obtained, roll-over occurs, T_e < 5 eV, ionisation front moves upstream (Fig. 2.)

✦ Used as an initial state for the ELM simulation

✦ Comparison to SOLPS [10], SOLPS results from [3]

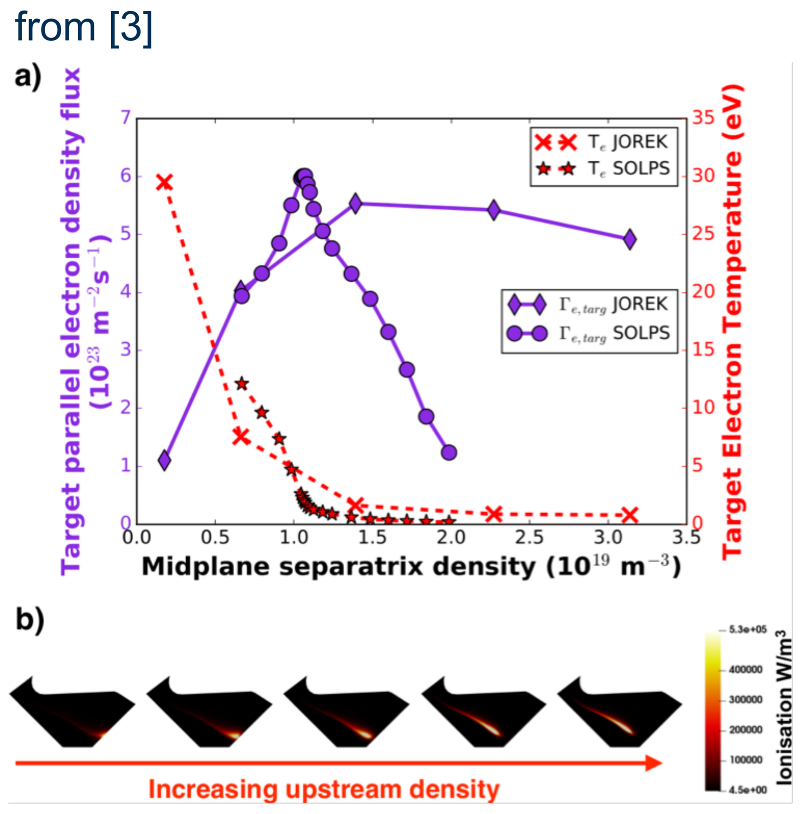

FIG. 2. (a) The target parallel electron density flux and target electron temperature as a function of upstream density, comparing JOREK with SOLPS [3]. (b) The ionisation front in the lower divertor, from the JOREK simulations.

4) Multiple toroidal mode number simulation

✦ MAST-U Super-X ELM simulation (n=2,4,6,..,20), evolution of energy of modes shown in Fig. 3. a)

✦ n=10 dominant when ELM crash occurs

✦ Evolution of the non-linear structure of the ELM filaments observed using the JOREK synthetic fast camera diagnostic (Fig. 3. b))

✦ Pedestal ELM thermal energy loss is 1.4 kJ. Simple analytical calculation shows ELM will burn-though divertor neutrals front

FIG. 3. (a) The evolution of the kinetic (coloured lines) energy of the mode numbers for the multi-mode simulation.
(b) The evolution of the filamentary structures during the multi-mode ELM simulation imaged with a synthetic fast camera diagnostic (t in ms).

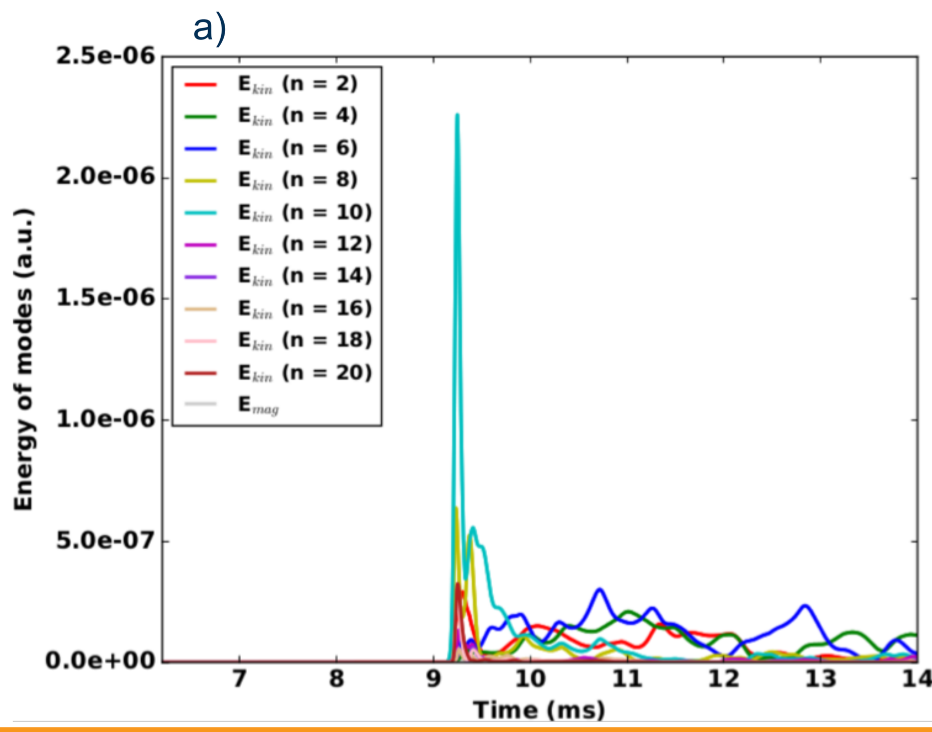

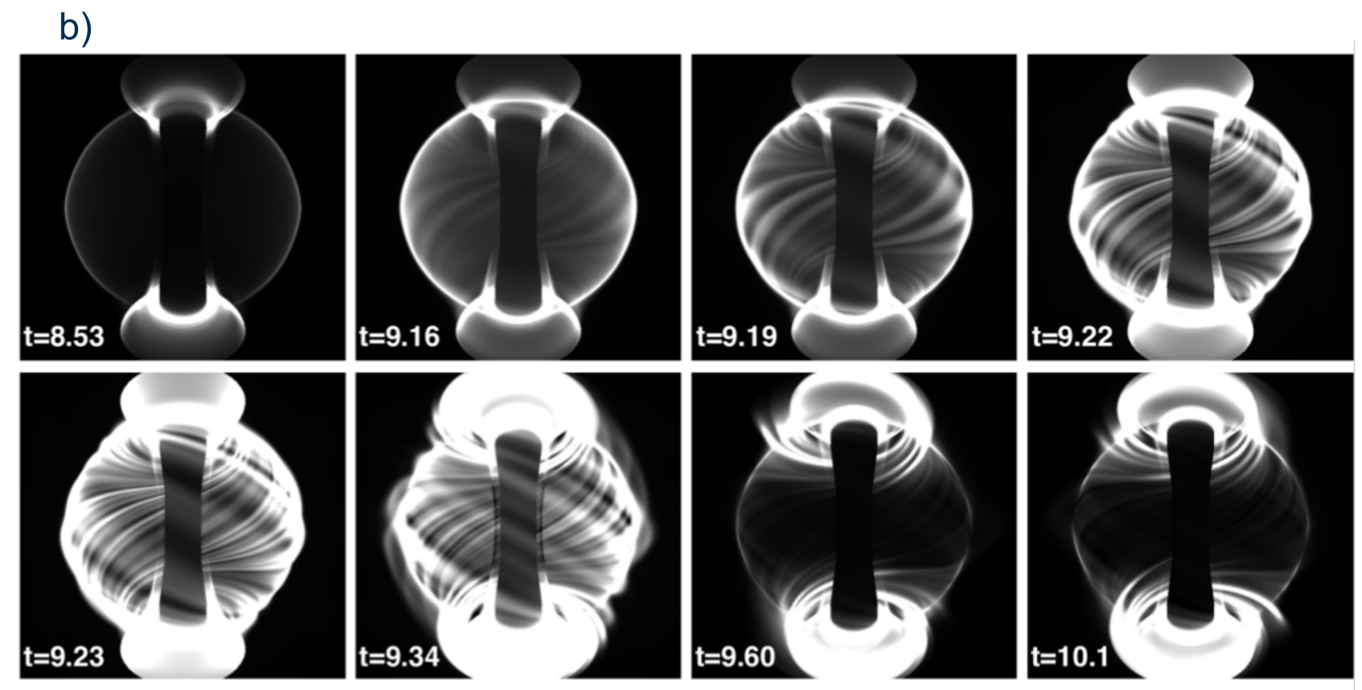

5) ELM burn-through in Super-X

✦ ELM burns through neutrals front in Super-X

✦ ELM q_{peak} to outer lower target is 9.8 MW/m^2 and factor 3 less to upper outer target (Fig. 4. a) and b)). Non-symmetric distribution to upper and lower divertors due to E×B rotation

✦ $\varepsilon_{||}$ is factor 46 lower than Eich ELM scaling (black diamond Fig. 1. g))

✦ Peak target T_e=150 eV and quickly recovers to almost pre-ELM conditions

✦ Recovery to almost pre-ELM conditions, in ~ 3 ms, which is shorter than type-I inter-ELM period for MAST (Fig. 4. a)-c))

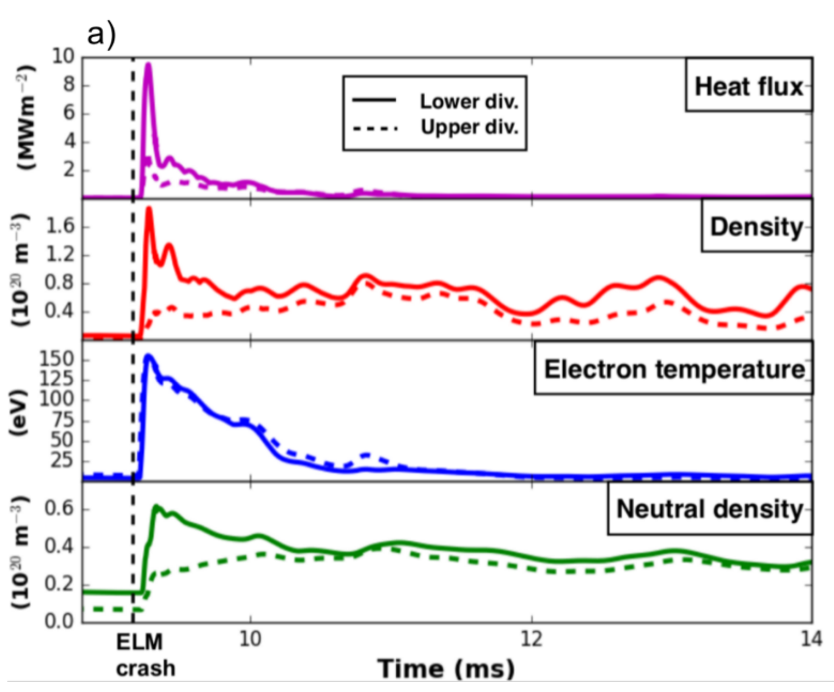

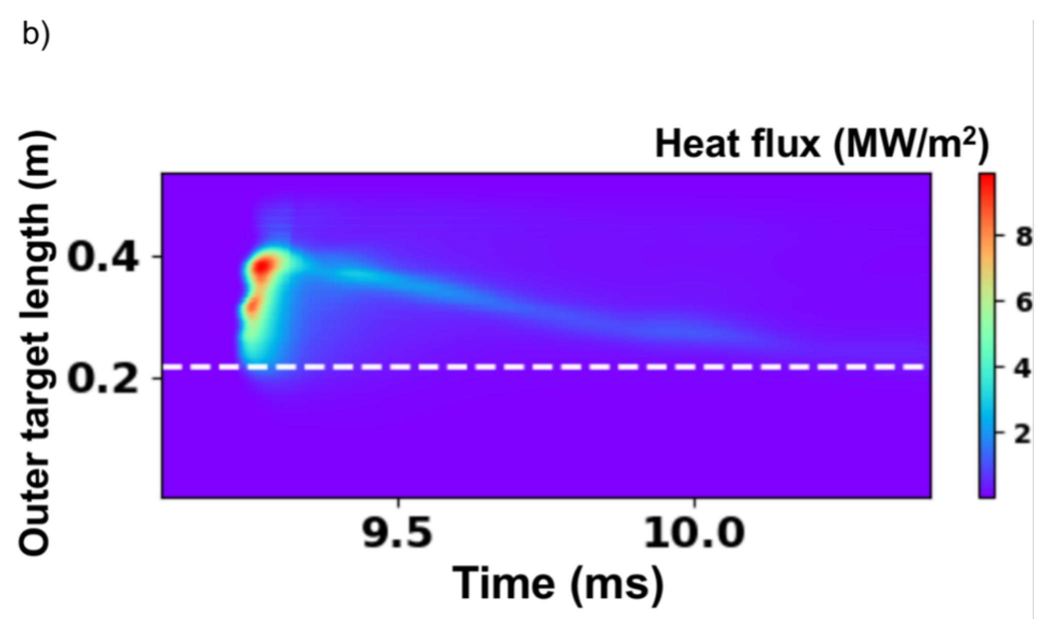

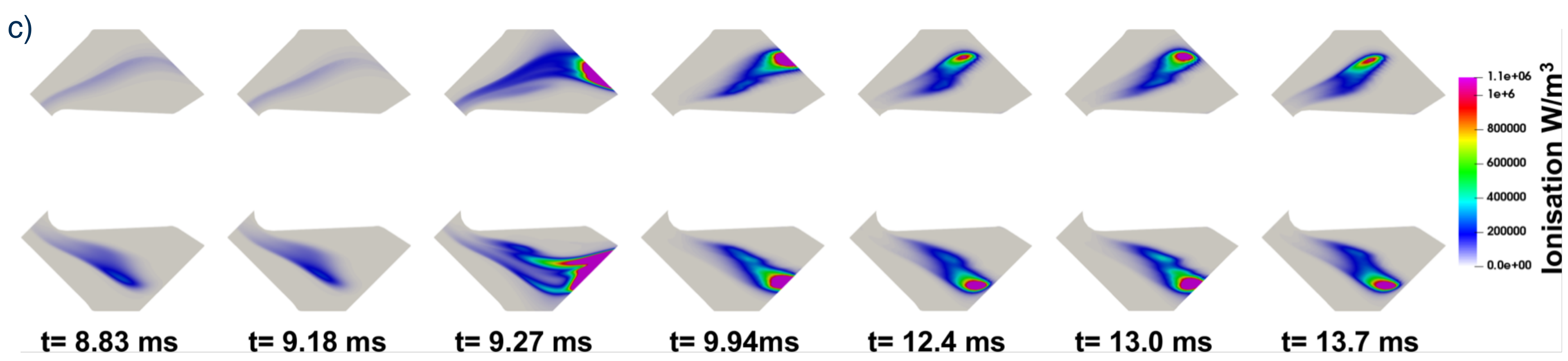

FIG. 4. (a) The evolution of the peak outer target values for the heat flux, density, electron temperature and neutral density for the upper (dashed lines) and lower (solid lines) divertors. (b) The heat flux pattern onto the Super-X lower outer target during the ELM simulation, zoomed in time to the peak heat flux to the target, from the ELM crash. White dashed line is the separatrix position. (c) The evolution of the ionisation fronts in the upper and lower outer Super-X divertors during the ELM simulation.

6) Summary

✦ Factor 11 reduction in q_{peak} to Super-X divertor

✦ Promising result for $\varepsilon_{||}$, with factor 46 reduction for Super-X. $\varepsilon_{||}$ ELM scaling may need modification for long legged and detached divertors

✦ ELM burns through neutrals front in Super-X but recovers to almost pre-ELM conditions

✦ Future work:
- include more physics such as diamagnetic flows
- advanced neutrals, SOL/divertor modelling [11], in JOREK, is in progress
- compare simulation results to MAST-U experimental data

References

[1] Fishpool G. et al 2013 J. Nucl. Mater. **438** S356–9
[2] Havlickova E. et al 2015 Plasma Phys. Control. Fusion **57** 115001
[3] Moulton D. et al 2017 44th EPS Conf. Plasma Physics (Belfast, UK, 26–30 June 2017) O5.129 (http://ocs.ciemat.es/EPS2017PAP/pdf/O5.129.pdf)
[4] Huysmans G.T.A. and Czarny O. 2007 Nucl. Fusion **47** 659–66
[5] Czarny O. and Huysmans G. 2008 J. Comput. Phys. **227** 7423–45
[6] Hoelzl M. et al Nuclear Fusion (submitted); preprint at: arXiv:2011.09120
[7] Smith S.F. et al Nucl. Fusion **60** (2020) 066021
[8] Pamela S.J.P. et al 2013 Plasma Phys. Control. Fusion **55** 095001
[9] Eich T. et al 2017 Nucl. Mater. Energy **12** 84–90
[10] Xavier B. et al 2016 Plasma Fusion Res. **11** 1403102–1403102
[11] S Korving, GTA Huijsmans et al, private communication

This work has been carried out within the framework of the EUROfusion Consortium and has received funding from the Euratom research and training programme 2014-2018 and 2019-2020 under grant agreement No 633053 and from the RCUK Energy Programme [grant number EP/P012450/1]. To obtain further information on the data and models underlying this paper please contact PublicationsManager@ukaea.uk*. The views and opinions expressed herein do not necessarily reflect those of the European Commission. Funding from the EPSRC Fusion CDT grant number EP/L01663X/1 is acknowledged.

CCFE CULHAM CENTRE FOR FUSION ENERGY

FUSION CDT

EPSRC Engineering and Physical Sciences Research Council

EUROfusion